

Why Coordinated Distributed Experiments Should Go Global

LAURA YAHDIJIAN¹, OSVALDO E. SALA, JUAN MANUEL PIÑEIRO-GUERRA, ALAN K. KNAPP, SCOTT L. COLLINS, RICHARD P. PHILLIPS, AND MELINDA D. SMITH

The performance of coordinated distributed experiments designed to compare ecosystem sensitivity to global-change drivers depends on whether they cover a significant proportion of the global range of environmental variables. In the present article, we described the global distribution of climatic and soil variables and quantified main differences among continents. Then, as a test case, we assessed the representativeness of the International Drought Experiment (IDE) in parameter space. Considering the global environmental variability at this scale, the different continents harbor unique combinations of parameters. As such, coordinated experiments set up across a single continent may fail to capture the full extent of global variation in climate and soil parameter space. IDE with representation on all continents has the potential to address global scale hypotheses about ecosystem sensitivity to environmental change. Our results provide a unique vision of climate and soil variability at the global scale and highlight the need to design globally distributed networks.

Keywords: climate change, climate–soil parameter space, coordinated–distributed experiments, drought, ecosystem sensitivity

All terrestrial ecosystems are being affected to some extent by alterations in climate, biogeochemistry, and disturbance regimes as a consequence of human activities (Vitousek et al. 1997, IPCC 2013, Flombaum et al. 2017). Indeed, the scope and pace of change occurring in ecological systems today—and forecasted for the future—are unprecedented in human history (IPCC 2013). Although there are many approaches ecologists may use to better understand how and why ecosystems respond to global changes, experiments have long been recognized as critical for identifying mechanisms underlying ecological responses (Rustad 2008, Smith 2011a, Beier et al. 2012). However, most manipulative experiments are conducted with different approaches and methods, making it challenging to determine whether the variation in ecological responses is due to different methodologies or to differences in key ecosystem attributes (Smith 2011a, Borer et al. 2014). Although syntheses and meta-analyses are useful tools for assessing broadscale drivers of change (Wu et al. 2011, Komatsu et al. 2019), the different methodologies used across studies can limit our ability to draw inferences (Gurevitch and Mengersen 2010). Consequently, knowledge of how and why ecosystems differ in their sensitivity to global changes remains poorly quantified because we lack an understanding of the mechanisms driven ecosystem responses. Network-level experiments with common research protocols and methodologies are increasingly being used to fill this gap (Beier et al. 2004, 2012, Smith 2011b, Vicca et al. 2012, Fraser et al. 2013,

Borer et al. 2014, Knapp et al. 2015a). However, their ability to shed insight on the ecosystem sensitivity to global change depends on the degree to which they cover a significant proportion of the global range of climate, soil, and vegetation variables.

Coordinated distributed experiments

Coordinated distributed experiments (*sensu* the Nutrient Network; Borer et al. 2014) go beyond unique, local-scale studies and have the potential to be important for understanding mechanisms underlying differential ecosystem sensitivity to global change (Peñuelas et al. 2007, Smith 2011a, Knapp et al. 2015a, Reinsch et al. 2017). Although coordinated approaches account for the fact that environmental parameters differ among locations, a global distribution of experiments may be required to encompass the full range of natural variability of climate and soil variables. As such, the success of a coordinated distributed experiment depends on the distribution of sites in soil–climate space. Experiments encompassing the full range of environmental variables have the possibility of testing the entire spectrum of ecosystem responses. In contrast, networks of experiments limited in parameter space may miss part of the response surface. Moreover, they may be severely constrained in their predictive power and in their ability of addressing global change questions.

A global distribution of experimental sites makes sense only if climate and soil variables differ among continents.

In the present article, we aimed to assess whether any single continent contains sufficient variation in climatic and soil parameters to allow for the testing of global hypotheses in selected regions or whether a full multicontinent approach is needed. As site locations in coordinated distributed experiments are generally established on the basis of voluntary willingness to participate, it is important to assess the realized representation of each of them.

Climate and soil parameter space

When analyzing the main environmental factors, we might conclude that almost all possible terrestrial climate and soil conditions are represented within a single large region or that multiple regions are required to encompass existing global patterns. For instance, several hypotheses indicate that aboveground net primary production sensitivity to precipitation amount depends on key climatic and edaphic variables related to fertility and soil–water availability (Yahdjian et al. 2011, Smith et al. 2017). These variables include mean annual precipitation (Huxman et al. 2004, Sala et al. 2012), mean annual temperature (Epstein et al. 1996), seasonality, which measures the synchrony between wet and warm seasons based on monthly data of precipitation and temperature (Sala et al. 1997, Saha et al. 2018), continentality or the temperature and monthly precipitation range. Also, soil characteristics that determine water-holding capacity, such as soil texture (Hanks and Ashcroft 1980), soil depth and slope (Fan et al. 2017), and soil organic carbon (Chapin et al. 2002) have been hypothesized as important variables dictating aboveground net primary production response per unit of precipitation. However, the environmental parameter space is usually described in terms of mean annual temperature and mean annual precipitation only, and the inclusion of other climate variables or soil attributes is much less common.

To assess the global range of environmental parameter space, we describe the global distribution of climatic and soil variables and identify the main differences among continents to establish a baseline against which the representativeness of global distributed experiments can be assessed. To do so, we constructed 95% confidence ellipses for a suite of environmental variables from global databases using the `plotGroupEllipses` function in R (R core Team 2018), and we estimated the overlap of the standard ellipses fitted by maximum likelihood using the `maxLikOverlap` function (SIBER package, R core Team 2018). This procedure allowed comparison among ellipses from continents with different number of data points (Jackson et al. 2011). We then estimated the area of each ellipse with the `siberConvexhull` function to quantify the range of variation within each continent. As a case study, we compared the environmental context of the International Drought Experiment (IDE, <http://drought-net.colostate.edu>; Smith et al. 2017) with the global range of environmental variation that occurs across continents. This coordinated distributed experiment is testing hypotheses about the control of ecosystem sensitivity to

extreme drought and how they vary globally among deserts, grasslands, shrublands, and forests. To determine how well the DroughtNet sites represent global variation, we assessed the environmental distribution of IDE sites within the globally defined environmental space (box 1).

Climate and soil data sources

Comparable climate and soil data are needed to describe the global physical–environmental space. We selected nine climatic and soil variables and extracted them from publicly available global data sets that ensure consistency across the globe (see table 1 for a complete list of variables and data sources). For each global terrestrial 1-degree pixel, we identified the appropriate continental region (i.e., North America, Central and South America, Europe, Africa, Asia, and Australia). Climate data were extracted from WorldClim's global climate data (version 1.4, available at www.worldclim.org), and loaded in R with a raster package for all terrestrial pixels. Mean annual values of total precipitation and temperature represent the long-term values (years 1960–1990) of terrestrial condition from WorldClim version 1.4, the most recent version for R (Hijmans et al. 2005).

Annual values of temperature and precipitation do not fully represent how environments vary seasonally. Therefore, water balance dynamics over seasonal time frames cannot be captured by climatic variables described at the annual scale. To address this deficiency, we calculated a measure of seasonality, in this case the overlap between wet and warm seasons, which was estimated by the Pearson correlation coefficient on monthly data of precipitation and temperature extracted from the same climate data source (Sala et al. 1997). As all Pearson correlation coefficients, seasonality values can be negative or positive and zero means no correlation. Seasonality ranges from -1 to 1 , and negative values describe Mediterranean climates with dry summers and rainy winters, whereas positive values correspond to sites with summer (warm season) precipitation (Kottek et al. 2006).

Continentality was estimated by the annual temperature range, which is the difference between maximum (hottest) and minimum (coldest) monthly temperature. Similarly, mean precipitation range represents the difference between the maximum and minimum monthly precipitation over the year, so large values of continentality or mean monthly precipitation range represent high variability in monthly temperature or precipitation. We also extracted and tested for other precipitation and temperature-related variables such as growing-season precipitation, precipitation of the warmest or wettest quarter, potential evapotranspiration, and the aridity index (the mean annual precipitation to potential evapotranspiration ratio) but discarded those variables because they were strongly correlated with mean annual precipitation or mean annual temperature (supplemental figure S1).

Soil texture, a categorical (unitless) variable, was extracted from the Hydrology Soil database (<http://iridl.ldeo.columbia>).

Box 1. Empirical evaluation of a globally distributed drought experiment.

The impact of drought on ecosystems depends on the magnitude of the precipitation anomaly and the relative response rate of ecosystems to drought (Seddon et al. 2016). Evidence showed that some ecosystems are relatively insensitive to short-term (e.g., 1 year) changes in precipitation, whereas others are highly sensitive and respond dramatically to similar drought events (Knapp et al. 2015). It is unclear if this observed differential sensitivity among ecosystems is a consequence of different ecological, climatic, and/or soil parameter space. A coordinated, distributed drought experiment (the “International Drought Experiment,” IDE, <http://drought-net.colostate.edu/>) was established to test hypotheses about the control of ecosystem sensitivity to extreme drought through a distributed rainfall manipulation experiment (Smith et al. 2017, Hilton et al. 2019). In this network, comparable drought treatments among the broad range of terrestrial ecosystems with disparate climates were achieved by simulating dry years with the same low probability of occurrence (once every 100 years; Lemoine et al. 2016, Knapp et al. 2017). To test hypotheses about the drivers of drought sensitivity, the network had to cover a representative portion of the climatic–soil parameter space. In the present article, we assessed the realized representation of IDE against the background of the global patterns generated in our analysis to evaluate how well experimental IDE sites through voluntary participation captured soil and climate gradients at the global scale described with our approach.

The IDE sites were those registered in the network data base (www.drought-net.org) and carrying out the same rainfall manipulation experiments (supplemental figure S2, supplemental table S5). We identified 127 sites covering the six continental regions and encompassing the hyper-arid through hyper-humid gradient of bioclimatic zones (Le Houérou 1996; table S5). Climate and soil data for the IDE locations were extracted from the same data bases used in this study (table 1). In addition, we extracted the Global Aridity index (mean annual precipitation to potential evapotranspiration ratio; a high value means low aridity), from the Global Aridity database (www.cgiar-csi.org/data/global-aridity-and-pet-database) to classify the experimental IDE sites along the arid–humid bioclimatic zones (Le Houérou 1996, table S5).

The IDE sites represent an even distribution of rainfall manipulation experiments in the mean annual temperature and mean annual precipitation space, specifically in the mean annual precipitation range between 0 and 2500 millimeters per year and mean annual temperature higher than -5 degrees Celsius (figure 1), which is also the most represented on Earth (the background in figure 1). The effects of climate change on ecosystem functioning depend on the interactions between climate events and ecosystem sensitivity to predicted climate changes (Sala et al. 2015). Our results provide insights about the potential of IDE to address questions regarding ecosystem responses to drought. The IDE network will advance our understanding on drought sensitivity that is imperative to assess future ecosystem functioning and the provisioning of ecosystem services.

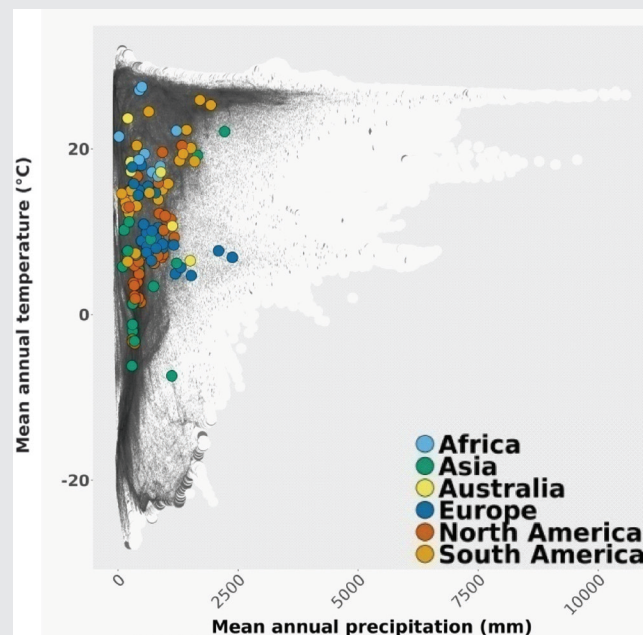


Figure 1. IDE coverage in global mean annual temperature as a function of mean annual precipitation. The background shows in a grayscale the representation of the global combinations of mean annual temperature and mean annual precipitation, where the range from white to dark grey and black depicts the density of pixels in the world with that combination of variables. The distribution of IDE sites is deployed with the same colors according to continents in figure 2.

Table 1. Climate and soil variables included in this analysis, defined in a globally consistent manner.

Climatic	Abbreviations	Units	Source	References
Mean annual precipitation	MAP	Millimeters per year	BIO12	WorldClim
Mean annual temperature	MAT	Degrees Celsius	BIO1	http://WorldClim.org
Seasonality (correlation)	SEASON	Unitless	–	
Continentality (temperature range)	CONT	Degree Celsius	BIO7(BIO5-BIO6)	
Monthly precipitation range	MPR	Millimeters	BIO13-BIO14	
Soil texture	TEXT	Unitless	Hydrology Soils Data set	http://iridl.ldeo.columbia.edu/SOURCES/.NASA/.ISLSCP/.GDSLAM/.HydrologySoils/.soils/.data_set_documentation.html
Soil depth	DEPTH	Meters		http://esdac.jrc.ec.europa.eu/ESDB_Archive/octop/octop_data/
Average slope	SLOPE	Percentage		
Soil organic carbon	SOC	Tons per hectare		

edu/SOURCES/.NASA/.ISLSCP/.GDSLAM/.Hydrology-Soils/.soils), a 1-degree grid resolution Soil Map of the World (Zobler 1986, FAO 1988). Texture is classified according to the relative size of soil particles, following the scheme proposed by Zobler (1986). Textural classes reflected the relative proportions of clay (fraction less than 2 micrometers), silt (2–50 micrometers), and sand (50–2000 micrometers) in the soil. The original FAO data used the terms *coarse*, *medium*, *fine*, or a combination of these terms on the basis of the relative amounts of clay, silt, and sand present in the top 30 centimeters (cm) of soil. Zobler (1986) converted these data into a 1-degree grid resolution array, and then assigned the common names sandy loam, sandy clay loam, loam, and clay loam, which correlated with the USDA soil texture triangle (table 1).

Soil depth was extracted from the soil profile thickness file (Webb et al. 1993) derived from information contained in volumes 2–10 of the FAO and UNESCO Soil Map of the World (FAO 1988). The average topographical slope (SLOPE) for each 1-degree \times 1-degree square was derived from data sets constructed by the Science and Applications Branch of the EROS Data Center in Sioux Falls, South Dakota (table 1). Soil organic carbon content was extracted from the Harmonized World Soil Database and values were expressed in tons of carbon per hectare (Nachtergaele et al. 2010, Hiederer and Köchy 2011). The resolution of soil organic carbon data was 30 arc seconds (approximately 1 kilometer for Ecuador), and two data sets were available, from 0–30 cm and 30–100 cm of soil depth. In the present article, we used only the 0–30 cm because it had a better resolution and is associated with the soil profile where plant roots concentrate (Jackson et al. 1996).

All climate data used for this study are available from WorldClim (global climate data, version 1.4, www.worldclim.org; global aridity database, www.cgiar-csi.org/data/global-aridity-and-pet-database; and soil data, <http://iridl.ldeo.columbia.edu/SOURCES/.NASA/.ISLSCP/.GDSLAM/.Hydrology-Soils/.soils>). To harmonize climate and soil data

sets, we used the coarse resolution of the Worldclim, 2.5 minutes (around 5 square kilometers).

Patterns in global environmental space

The terrestrial climate space determined by the joint combination of macroclimatic parameters mean annual temperature versus precipitation had a triangular shape, as was proposed by Whittaker (1975), resulting from the spherical configuration of Earth that creates a larger area and precipitation–temperature combinations around the tropics than in polar regions (figure 2a). There was an interaction between mean annual precipitation and mean annual temperature values (figure 2a; Koenig 2002). The wettest regions in the warmest climates have more energy to fuel the water cycle. Consequently, the mean annual temperature range was broader in drier regions of the world (figure 2a). However, there were differences in mean annual temperature and precipitation among continents (figure 2a) and very low overlap among the six continents (ellipses in figure 2b, table 2, supplemental table S1).

The global seasonality of precipitation was evenly distributed on the basis of mean annual precipitation (figure 3a). Winter and summer precipitation regimes (negative and positive correlations, respectively) were equally represented in the 0–3000 millimeters range of mean annual precipitation, but extreme seasonality was less common in locations with higher mean annual precipitation rate (figure 3a). Different continents had distinct seasonality patterns (figure 3d, supplemental table S2). For example, South America had a large representation of winter precipitation and low seasonality sites that were not represented in either North America or Europe (figure 3d). Continentality showed a global pattern of decreasing temperature range with increasing mean annual precipitation and wettest regions located in low continental (low temperature range) climates (figure 3b). In other words, sites located far from the oceans, and therefore with high continentality, tended to have lower precipitation compared with maritime regions.

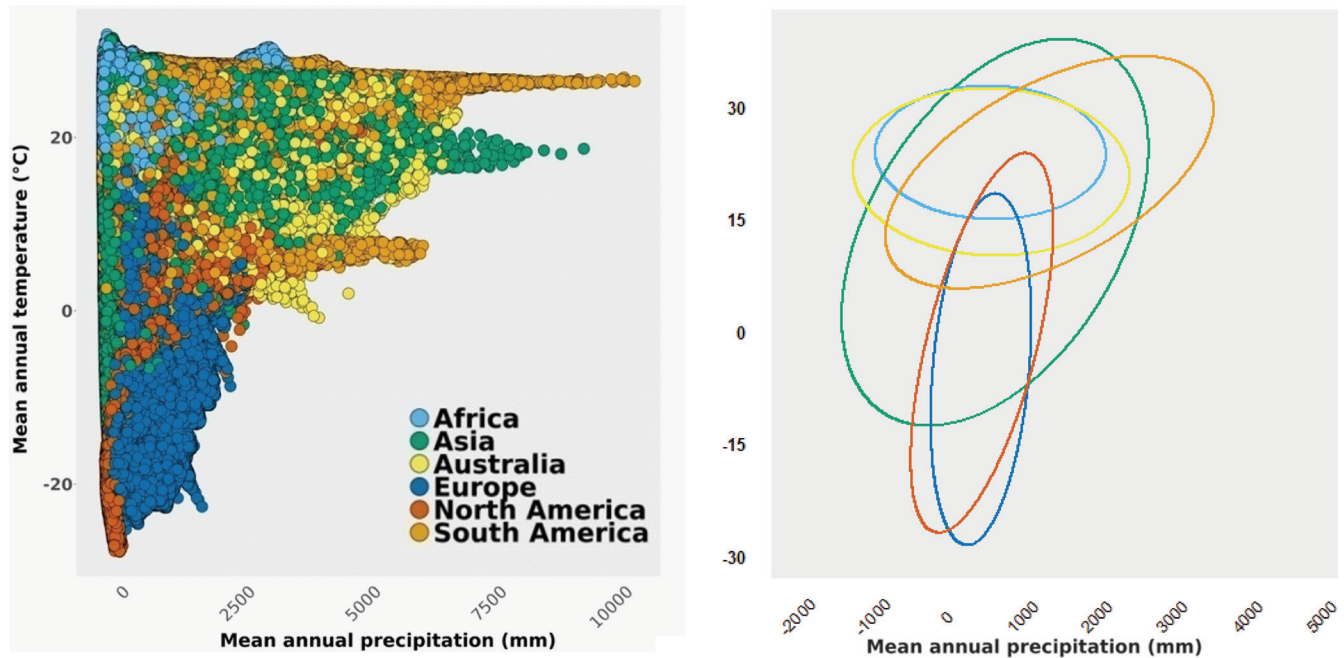


Figure 2. Global mean annual temperature as a function of mean annual precipitation, with colors representing the six continents. (a) The dots represent a pixel of terrestrial area depicted according to each continent. (b) 95% confidence ellipses estimated by maximum likelihood using the *maxLikOverlap* function (*SIBER* package in R).

It is important to highlight that there were large differences in temperature ranges among continents (figure 3e, supplemental table S3). In the Southern Hemisphere, high continentality is extremely rare because of the smaller land-masses in the middle latitudes and nearly absent of land at 40–60 degrees south. By contrast, North America and Asia in the Northern Hemisphere showed higher temperature ranges (over 30 degrees Celsius), whereas Europe and Australia showed intermediate values. Africa and South America exhibited the lowest continentality (figure 3e). The monthly precipitation range showed a strong correlation with mean annual precipitation, with monthly precipitation range increasing with mean annual precipitation (figure 3c). A clear continental pattern emerged from this climate space with Asia and South America showing higher monthly precipitation range than Europe and North America (figure 3f, supplemental table S4).

The global pattern of soil properties showed no correlation between mean annual precipitation and texture (figure 4a) or soil depth (figure 4b). All types of soil texture were spread along the arid–humid mean annual precipitation gradient with Australian sites showing coarser soils and South American sites largely represented in the loam and clay soil textural classes (figure 4a). Soil slope showed that globally, flat and low-slope soils were more represented on earth than slopes higher than 30% without a continental pattern (figure 4c). The soil organic carbon in the 0–30 cm depth showed a slightly positive correlation with mean annual precipitation and a broader soil organic carbon range in

drier regions, with South America region more varied for soil organic carbon and mean annual precipitation than the other continents (figure 4d).

The multivariate analysis of terrestrial climate and soil variables highlights the global distribution of these variables among continents (figure 5). The plane defined by the first two principal components accounted for 42% of the variance. The first principal component included sites tending to have high mean annual temperature or mean annual precipitation on one end and large seasonality and continentality on the other end (figure 5). The second principal component included soil variables, and range from low to high slope, depth, and soil organic carbon (arrows in figure 5). The ellipses delineated continent patterns and clearly demonstrate that no single continent covers the integrated global climate–soil space (figure 5). Continental patterns stress the necessity of a global network given that no single continent covers the integrated climate–soil space (table 2).

Implications

Coordinated distributed experiments provide a framework for both comparing ecosystem sensitivity to global-change drivers and for identifying the mechanisms that underlie those responses. However, the ability of coordinated networks to shed insight on fundamental drivers of ecosystem dynamics depends on whether the location of the experiments cover a significant proportion of the global range of climate, soil, and vegetation variables. The pattern of macro-climatic variables mean annual precipitation, mean annual

Table 2. Percentage of bivariate climate variables depicted in figures 2 and 3 and of PCA in Figure 5, accounted for by each continent.

Climatic	MAT	SEASON	CONT	MPR	PCA
Africa	30	40	26	16	49
Asia	74	79	77	73	81
Australia	45	68	34	22	45
Europe	48	42	41	4	46
North America	48	37	34	8	48
South America	69	84	50	34	55

Note: Each variable listed was deployed against mean annual precipitation (MAP). See abbreviation and units of each climate variable in table 1. The last column refers to the area of the 95% confidence ellipses in principal component space depicted in figure 5. Abbreviations: CONT, continentality; MAT, mean annual temperature; MPR, monthly precipitation range; PCA, principal component analysis.

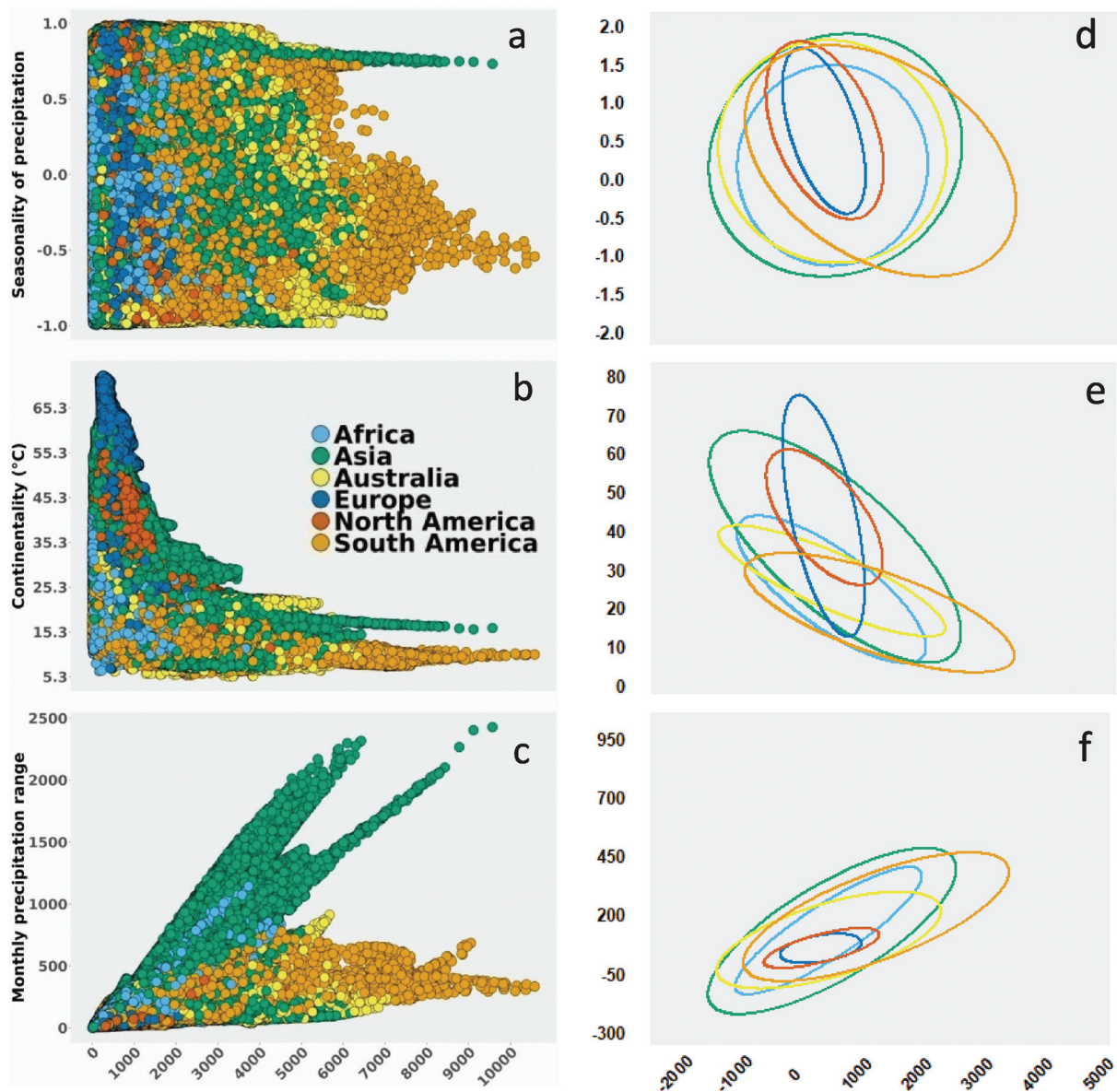


Figure 3. Global distribution of climatic variables as a function of mean annual precipitation in the six continental masses. (a, d) Seasonality index showing the overlap between wet and warm seasons, calculated as the Pearson correlation coefficient between monthly precipitation and temperature (unitless). (b, e) Continentality based on temperature range estimated as the difference between maximum (hottest) and minimum (coldest) monthly temperature. (c, f) Monthly precipitation range estimated as the difference between the maximum and minimum monthly precipitation over the year. Panels (d), (e), and (f) contain 95% confidence ellipses estimated by maximum likelihood using the maxLikOverlap function (SIBER package in R).

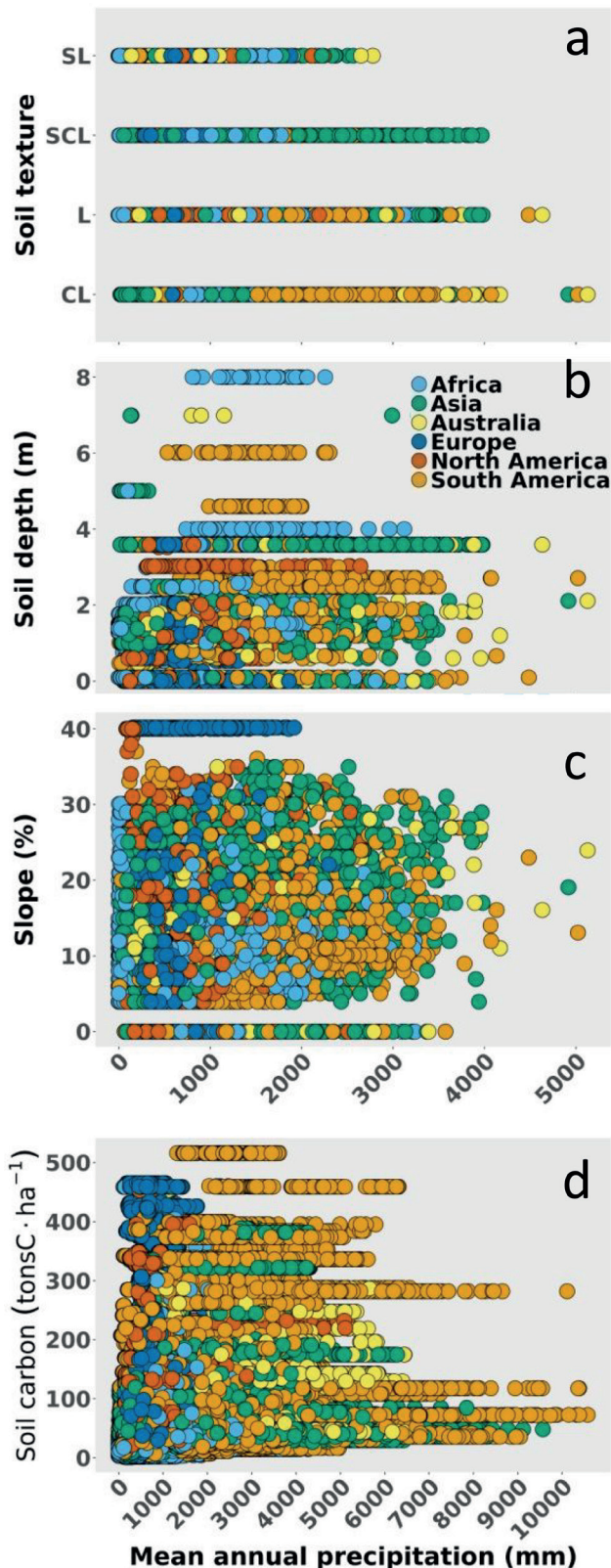


Figure 4. Global distribution of soil variables as a function of mean annual precipitation. (a) Soil texture, (b) soil depth, (c) slope, and (d) soil carbon content (tons of carbon per hectare). Texture classes in panel (a) are abbreviated CL, clay loam; L, loam; SCL, sandy clay loam; SL, sandy loam.

temperature, and continentality that measured the temperature range, showed important distinctions among continents that emphasize the necessity of a global network to account for differences in climate. Indeed, the soil–climate integration space described by the multivariate analysis of climatic and soil variables showed that six continental regions of the world are needed to cover the full combination of different climate and soil variables in Earth’s terrestrial ecosystems.

Global patterns of climate were related to the spherical shape of the Earth and the uneven distribution of continental masses relative to water in Northern and Southern Hemispheres (Akin 1991, Chapin et al. 2002). Soil characteristics modulate water infiltration, water storage, water potential, and soil fertility, all of which affect plant responses to precipitation change (Smith et al. 2017). Soil variables represent another dimension of the physical space that also determines ecosystem functioning. In contrast with the observed differences in climate variables, no continental patterns emerged in soil variables. This global analysis confirmed previous studies of aboveground net primary production controls at the subcontinental scale showing that climate variables changed at a coarser scale than soil variables (Sala et al. 1988). A study of aboveground net primary production of more than 900 sites in North America captured the climate effect when those sites were lumped into 100 larger units but needed to be disaggregated to evaluate the effect of soil texture on productivity (Sala et al. 1988). Therefore, distributed experiments may need to encompass large-scale climate patterns as well as finer scale soil patterns.

Our analyses serve as a basis for the design and deployment of future coordinated distributed experiments, and they provide an underlying mechanism to evaluate the generality of conclusions from existing global experimental networks. As the analysis represents a spatial description of the terrestrial environmental parameter space, the range of variation of climate variables is wider than the expected by climate change because it covers the full extent of global variation. In addition, our approach identified the main factors that capture the global variability of the physical–environmental space, including not only the macroclimatic variables mean annual precipitation and mean annual temperature, but additional climate and soil variables that also control the functioning of ecosystems and their response to different global-change drivers (Flombaum et al. 2017). Finally, our framework is based on a data-driven approach and publicly available sources of information, so it could be applied to assess the representativeness of environmental observatory networks and complement previous assessments at the national scale (Villarreal et al. 2018, Villarreal et al. 2019).

Most coordinated distributed experiments have a national or continental extent or cover a specific biome or climate type (Beier et al. 2004, Fraser et al. 2013, Borer et al. 2014a, Maestre and Eisenhauer 2019). Many of them use coarse grids, sample locations in some regions and often do not

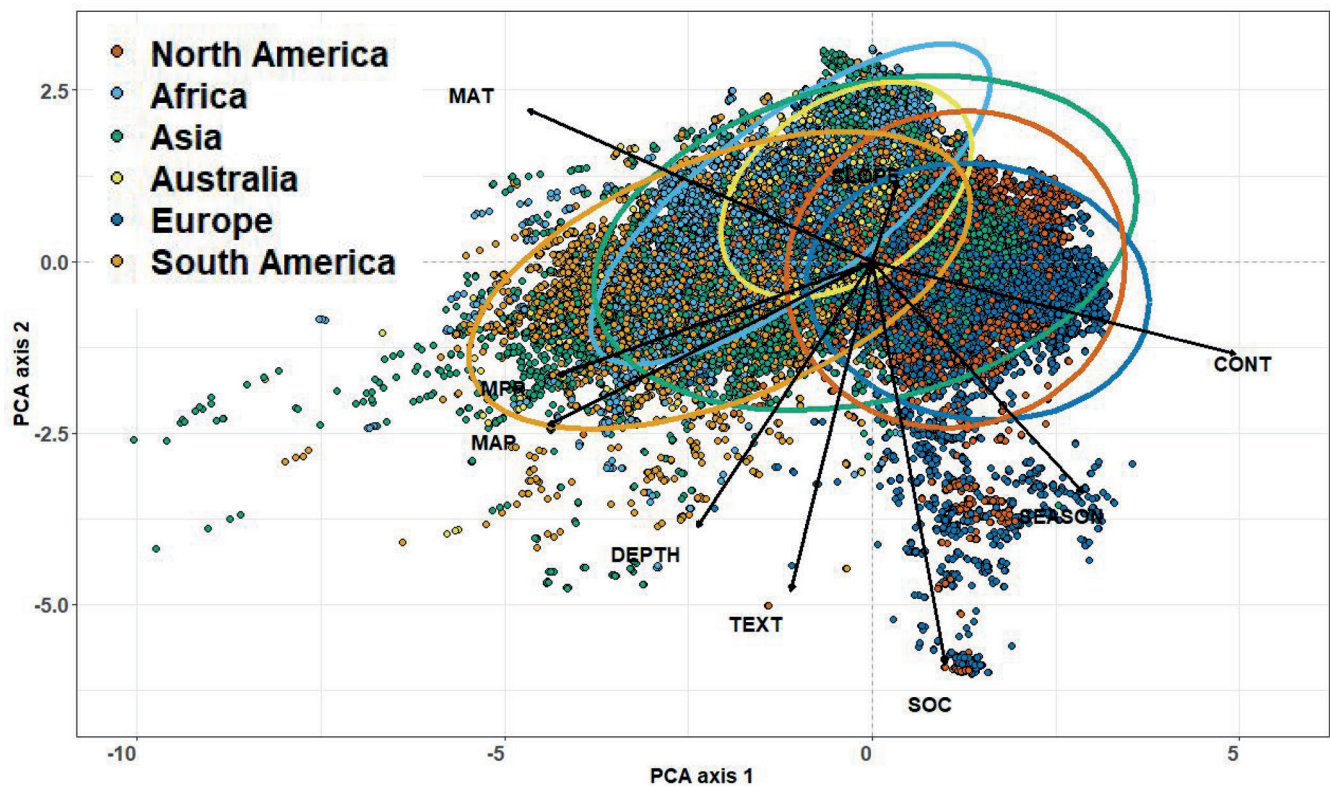


Figure 5. Soil-climate space as depicted by a principal component analysis (PCA) showing continental representation (the colored dots). The plane defined by the first two principal components accounted for 42% of the variance. PCA axis 1 included sites ranging from high mean annual temperature (MAT) or mean annual precipitation (MAP) on one end and large seasonality (SEASON) and continentality (CONT) on the other end. PCA axis 2 included soil variables and ranges from low to high slope, depth and soil organic carbon (SOC). Solid arrows indicate direction and weighing of vectors representing the relative contribution of the five climate and four soil parameters considered (table 1). The 95% confidence ellipses represent data clusters in the PCA by continents (Fox and Weisberg 2011). Variables are described in table 1 and the percent cover of the ellipses accounted for by each continent area is informed in the last column of table 2.

span the whole north to south gradient or lack extreme environments. Moreover, most coordinated distributed experiments, including the International Drought Experiment (IDE), did not have an a priori design but instead were built on voluntary participation from around the world. Consequently, they are often biased toward regions with the highest concentrations of scientist and resources such as North America and Europe (Wu et al. 2011). Our analysis highlighted the importance of deploying coordinated distributed experiments that widely represent the environmental parameter space, with the understanding that different networks may need different configurations depending on the type of questions that they address. Our sampling approach implied a spatial integration of data into grid cells, and therefore, the results can mask heterogeneous physical conditions that occur at smaller scales. The result may suggest that these scale differences may be more important for soil variables than climate variables.

In conclusion, this study represents a step forward in the analysis of climate and soil parameter space that can be useful in the design of distributed experimental networks,

which are increasingly being developed to address large-scale ecological questions. Coordinated distributed experiments may benefit from a design that captures as much as possible the full extent of global variation in climate and soil parameter space, which admittedly may be challenging to achieve in some extreme environments. The latitudinal changes in most environmental variables and the different patterns in the Northern versus Southern hemisphere because of the land-ocean ratio stress the importance of widening the coverage of the parameter space. Generally, climate change will result in drier climates in dry regions and wetter climate in wetter regions. As a consequence, the development or expansion of existing coordinated global networks need to be cognizant of zones of rapidly changing climate or hot spots of climate change as priorities of inclusion into these networks wherever possible. The expected changes in climate in the next 50–100 years will have huge implications for ecosystems and human wellbeing but will be small relative to the spatial gradient described in the present article. Nevertheless, our results provide a unique vision of climate and soil variability at the global scale and highlight

the need to consider global patterns of climate and soil variables as much as possible when designing coordinated distributed experiments.

Acknowledgments

This work was supported by US National Science Foundation Research Coordination Network grants no. DEB 1354732, no. DEB 1754106, and Jornada LTER no. DEB 2025166; Arizona State University Global Drylands Center; and Argentina grants no. PICT 2014–3026, no. PICT 2015–2827, and no. CONICET PIP 2015–0709. JMP was supported by a postdoctoral fellowship from IAI-CRN 3005. We thank the Drought-Net steering committee for fruitful discussions.

Supplemental material

Supplemental data are available at *BIOSCI* online.

References cited

- Akin WE. 1991. *Global Patterns: Climate, Vegetation, and Soils*. University of Oklahoma Press.
- Beier C, et al. 2012. Precipitation manipulation experiments: Challenges and recommendations for the future. *Ecology Letters* 15: 899–911.
- Beier C, et al. 2004. Novel approaches to study climate change effects on terrestrial ecosystems in the field: Drought and passive nighttime warming. *Ecosystems* 7: 583–597.
- Borer ET, Harpole WS, Adler PB, Lind EM, Orrock JL, Seabloom EW, Smith MD. 2014a. Finding generality in ecology: A model for globally distributed experiments. *Methods in Ecology and Evolution* 5: 65–73.
- Borer ET, et al. 2014b. Herbivores and nutrients control grassland plant diversity via light limitation. *Nature* 508: 517–520.
- Chapin FS III, Matson PA, Mooney HA. 2002. *Principles of Terrestrial Ecosystem Ecology*. Springer.
- Epstein HE, Lauenroth WK, Burke IC, Coffin DP. 1996. Ecological responses of dominant grasses along two climatic gradients in the Great Plains of the United States. *Journal of Vegetation Science* 7: 777–788.
- Fan Y, Miguez-Macho G, Jobbágy EG, Jackson RB, Otero-Casal C. 2017. Hydrologic regulation of plant rooting depth. *Proceedings of the National Academy of Sciences* 114: 10572–10577.
- Food and Agriculture Organization. 1988. *UNESCO soil map of the world, revised legend*. World Resources Report 60: 138.
- Flombaum P, Yehdjian L, Sala OE. 2017. Global-change drivers of ecosystem functioning modulated by natural variability and saturating responses. *Global Change Biology* 23: 503–511.
- Fox J, Weisberg S. 2011. *An R Companion to Applied Regression*. Sage.
- Fraser LH, et al. 2013. Coordinated distributed experiments: An emerging tool for testing global hypotheses in ecology and environmental science. *Frontiers in Ecology and the Environment* 11: 147–155.
- Gurevitch J, Mengersen K. 2010. A statistical view of synthesizing patterns of species richness along productivity gradients: Devils, forests, and trees. *Ecology* 91: 2553–2560.
- Hanks RJ, Ashcroft GL. 1980. *Applied Soil Physics: Advanced Studies*. Agricultural Science. Springer.
- Hiederer R, Köchy M. 2011. Global soil organic carbon estimates and the harmonized world soil database. *EUR* 79: 10–2788.
- Hijmans RJ, Cameron SE, Parra JL, Jones PG, Jarvis A. 2005. Very high resolution interpolated climate surfaces for global land areas. *International Journal of Climatology* 25: 1965–1978.
- Hilton TW, Loik ME, Campbell JE. 2019. Simulating International Drought Experiment field observations using the Community Land Model. *Agricultural and Forest Meteorology* 266–267: 173–183.
- Huxman TE, et al. 2004. Convergence across biomes to a common rain-use efficiency. *Nature* 429: 651–654.
- [IPCC] Intergovernmental Panel on Climate Change. 2013. *Climate Change 2013: The Physical Science Basis*. Cambridge University Press.
- Jackson RB, Canadell J, Ehleringer JR, Mooney HA, Sala OE, Schulze ED. 1996. A global analysis of root distributions for terrestrial biomes. *Oecologia* 108: 389–411.
- Jackson AL, Parnell AC, Inger R, Bearhop S. 2011. Comparing isotopic niche widths among and within communities: SIBER—Stable Isotope Bayesian Ellipses in R. *Journal of Animal Ecology* 80: 595–602.
- Knapp AK, et al. 2017. Pushing precipitation to the extremes in distributed experiments: Recommendations for simulating wet and dry years. *Global Change Biology* 23: 1774–1782.
- Knapp AK, et al. 2015a. Characterizing differences in precipitation regimes of extreme wet and dry years: Implications for climate change experiments. *Global Change Biology* 21: 2624–2633.
- Knapp AK, Carroll CJW, Denton EM, La Pierre KJ, Collins SL, Smith MD. 2015b. Differential sensitivity to regional-scale drought in six central US grasslands. *Oecologia* 177: 949–957.
- Koenig WD. 2002. Global patterns of environmental synchrony and the Moran effect. *Ecography* 25: 283–288.
- Komatsu KJ, et al. 2019. Global change effects on plant communities are magnified by time and the number of global change factors imposed. *Proceedings of the National Academy of Sciences* 116: 17867–17873.
- Kottek M, Grieser J, Beck C, Rudolf B, Rubel F. 2006. World map of the Köppen-Geiger climate classification updated. *Meteorologische Zeitschrift* 15: 259–263.
- Le Houérou HN. 1996. Climate change, drought and desertification. *Journal of Arid Environments* 34: 133–185.
- Lemoine NP, Sheffield J, Dukes JS, Knapp AK, Smith MD. 2016. Terrestrial precipitation analysis (TPA): A resource for characterizing long-term precipitation regimes and extremes. *Methods in Ecology and Evolution* 7: 1396–1401.
- Maestre FT, Eisenhauer N. 2019. Recommendations for establishing global collaborative networks in soil ecology. *Soil Organisms* 91: 73–85.
- Nachtergaele F, et al. 2010. The harmonized world soil database. Pages 34–37 in Gilkes R, Prakongkep N, eds. *Proceedings of the 19th World Congress of Soil Science, Soil Solutions for a Changing World*. International Union of Soil Sciences.
- Peñuelas J, et al. 2007. Response of plant species richness and primary productivity in shrublands along a north–south gradient in Europe to seven years of experimental warming and drought: Reductions in primary productivity in the heat and drought year of 2003. *Global Change Biology* 13: 2563–2581.
- R Core Team. 2018. *R: A Language and Environment for Statistical Computing*. R Foundation for Statistical Computing. www.R-project.org.
- Reinsch S, et al. 2017. Shrubland primary production and soil respiration diverge along European climate gradient. *Scientific Reports* 7: 43952.
- Rustad LE. 2008. The response of terrestrial ecosystems to global climate change: Towards an integrated approach. *Science of the Total Environment* 404: 222–235.
- Saha MV, Scanlon TM, D'Odorico P. 2018. Climate seasonality as an essential predictor of global fire activity. *Global Ecology and Biogeography* 28: 198–210.
- Sala OE, Parton WJ, Lauenroth WK, Joyce LA. 1988. Primary production of the central grassland region of the United States. *Ecology* 69: 40–45.
- Sala OE, Lauenroth WK, Golluscio RA. 1997. Plant functional types in temperate semi-arid regions. Pages 217–233 in Smith TM, Shugart HH, Woodward FI, eds. *Plant Functional Types: Their Relevance to Ecosystem Properties and Global Change*. Cambridge University Press.
- Sala OE, Gherardi LA, Peters DPC. 2015. Enhanced precipitation variability effects on water losses and ecosystem functioning: Differential response of arid and mesic regions. *Climatic Change* 131: 213–227.
- Sala OE, Gherardi L, Reichmann L, Jobbágy E, Peters D. 2012. Legacies of precipitation fluctuations on primary production: Theory and data synthesis. *Philosophical Transactions of the Royal Society B* 367: 3135–3144.

- Seddon AWR, Macias-Fauria M, Long PR, Benz D, Willis KJ. 2016. Sensitivity of global terrestrial ecosystems to climate variability. *Nature* 531: 229–232.
- Smith MD. 2011a. An ecological perspective on extreme climatic events: A synthetic definition and framework to guide future research. *Journal of Ecology* 99: 656–663.
- Smith MD. 2011b. The ecological role of climate extremes: Current understanding and future prospects. *Journal of Ecology* 99: 651–655.
- Smith MD, Wilcox KR, Power SA, Tissue DT, Knapp AK. 2017. Assessing community and ecosystem sensitivity to climate change—toward a more comparative approach. *Journal of Vegetation Science* 28: 235–237.
- Vicca S, Gilgen AK, Camino Serrano M, Dreesen FE, Dukes JS, Estiarte M, Granier A. 2012. Urgent need for a common metric to make precipitation manipulation experiments comparable. *New Phytologist* 195: 518–522.
- Villarreal S, Guevara M, Alcaraz-Segura D, Brunsell NA, Hayes D, Loescher HW, Vargas R. 2018. Ecosystem functional diversity and the representativeness of environmental networks across the conterminous United States. *Agricultural and Forest Meteorology* 262: 423–433.
- Villarreal S, Guevara M, Alcaraz-Segura D, Vargas R. 2019. Optimizing an Environmental Observatory Network Design Using Publicly Available Data. *Journal of Geophysical Research: Biogeosciences* 124: 1812–1826.
- Vitousek PM, Mooney H, Lubchenco J, Melillo JM. 1997. Human Domination of Earth's Ecosystems. *Science* 277: 494–499.
- Webb RS, Rosenzweig CE, Levine ER. 1993. Specifying land surface characteristics in general circulation models: Soil profile data set and derived water-holding capacities. *Global Biogeochemical Cycles* 7: 97–108.
- Whittaker RH. 1975. *Communities and Ecosystems*. MacMillan.
- Wu Z, Dijkstra P, Koch GW, Peñuelas J, Hungate BA. 2011. Responses of terrestrial ecosystems to temperature and precipitation change: A meta-analysis of experimental manipulation. *Global Change Biology* 17: 927–942.
- Yahdjian L, Gherardi L, Sala OE. 2011. Nitrogen limitation in arid-subhumid ecosystems: A meta-analysis of fertilization studies. *Journal of Arid Environments* 75: 675–680.
- Zobler L. 1986. A World Soil File for Global Climate Modeling. National Aeronautics and Space Administration. Technical memo no. 87802.

Laura Yahdjian (yahdjian@agro.uba.ar) is an independent researcher with IFEVA-CONICET and an assistant professor in the Ecology Department at Faculty of Agronomy at the University of Buenos Aires, Argentina. Osvaldo Sala is a Regents' Professor in the School of Life Sciences and the School of Sustainability and is the director of the Global Drylands Center at Arizona State University, in Tempe, Arizona, United States. Juan Manuel Piñero-Guerra is a postdoc at Centro de Ciências Exatas e da Natureza, in the Departamento de Sistemática e Ecologia, Laboratório de Ecologia Aplicada e Conservação, Cidade Universitária, at the Universidade Federal da Paraíba, in João Pessoa, Brazil. Alan Knapp is a senior ecologist and professor at Colorado State University, in Fort Collins, Colorado, United States. Melinda Smith is a professor in the Department of Biology and the director of the Semiarid Grassland Research Center, at Colorado State University, in Fort Collins, Colorado, United States. Scott Collins is a distinguished professor in the Department of Biology at the University of New Mexico, in Albuquerque, New Mexico, United States. Richard P. Phillips is an associate professor and the director of research for the IU Research and Teaching Preserve, in the Department of Biology at Indiana University, in Bloomington, Indiana, in the United States.